Progress in the biomechatronic design and control of a hand prosthesis

Xinqing Wang, Yiwei Liu, Dapeng Yang, Nan Li, Li Jiang, Hong Liu

Abstract—A five-fingered, multi-sensory biomechatronic hand with sEMG interface is presented. The cambered palm is specially designed to enhance the stability while grasping. The location of the thumb is designed by maximizing interaction area between the thumb and other fingers. The opposite thumb could grasp along a cone surface, while maintaining its function. By taken the advantage of coupling linkage mechanism, each finger with three phalanges could fulfill flexion-extension movement independently. Besides, each finger is equipped with torque and position sensors. Thus, the cosmetics and dexterity are improved remarkably compared to conventional prosthesis. The hardware architecture is divided into control system and EMG signal processing system. Moreover, a novel two-stage decision strategy combing the position-based impedance control scheme is implemented to realize the real-time sEMG control of the hand. According to the grasp experiment results, the hand can accomplish several grasp modes stably; the success rate of 10 modes is up to 90%.

I. INTRODUCTION

PROSTHETIC hand as a branch of robotic research is widely addressed in the field of rehabilitation technologies. Commercial prostheses usually have simple structure and rarely no sensory system. These limitations deeply affect the functionality of hand, such as OTTOBOCK Hand [1]. Due to the drawbacks of commercial prostheses, many experimental prostheses with more degree of freedoms (DOFs) and sensors have been developed, such as FZK Hand [2], RTRII Hand [3], SDM hand [4], and Smarthand [5]. But these are still far away from being accepted as part of the body by the amputees.

Despite of several research effort aimed at innovating humanoid hand technology, surveys on the relevant functionality of the hand prosthesis with regard to daily use activities show that the main concerns of the amputees are aesthetics (62%), excessive weight (58%), lack of functional capabilities (50%); on the other hand, the opinions from rehabilitation professionals reveal that tactile bio-feedback is preferred largely [6].

The EMG signal is a fairy reliable measure of muscle activities and is widely used in prosthetic hand control for several decades. Many methods have been developed, which can be seen from our previous work, such as neural network [7] and Autoregressive model [8], but these methods are not quite similar with that of human hand and only 3 finger motions can be classified. In order to improve prehensile posture and success rate, advanced machine learning algorithm is required, such as Support Vector Machine which is a useful technique for data classification.

Further more; the objective of prosthetic hand control is not restricted within motion tracking in free space. Meanwhile, more work should be done to adopt intelligent force control methods which can be applied for regulating the grasp force. So, the research focuses on the compromise approach to develop a multi-fingered hand which can be controlled by intuitive myo-control scheme in the real-time. Its function and appearance are very close to the human hand.

II. MECHANICAL STRUCTURE

Since we intend to develop a hand mainly used as prosthetic device, the functionality, the interface with human beings, the cosmetics and weight, are important criteria which should be taken into account. The comparison between the prosthetic hand and human hand is shown in Fig. 1.
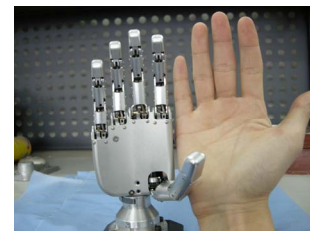

Fig. 1. The comparison between the prosthetic hand and human hand

The hand is 79mm wide, 159mm long and 21mm thick (when in full outspread), weighs about 420g including circuit boards. It is about 90% to a human hand out of consideration for inconspicuous. The hand is composed of five active fingers. Each finger is actuated by a DC motor independently. By taking the advantage of coupling mechanism, each finger is capable of rotate around the metacarpophalangeal (MCP), proximal interphalangeal (PIP), and distal interphalangeal (DIP) joints for a total of 15 movable joints of the entire hand. Compared with those of fixed shape fingers; this kind of design enhances the functionality of the hand and mimics the motion of human finger. The research ideology is described in detail in the following sections.

A. Configuration of Palm

According to traditional anatomical definitions, the human palm is comprised of three arches providing the necessary stability and mobility in the hand [9], these are distal

transverse arch, longitudinal arch and oblique arch.

In order to imitate the distal transverse arch, the cambered palm is designed which is far different from that of plain ones. The placement of each finger is shown in Fig. 2.
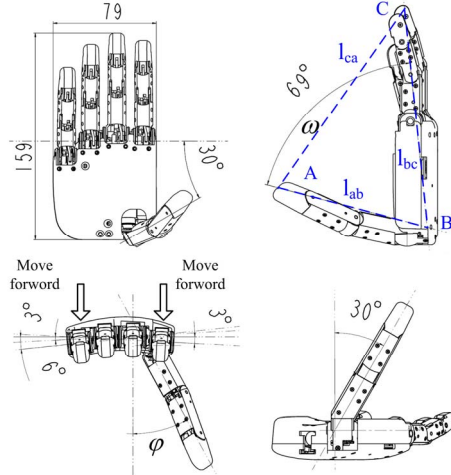

Fig. 2. Structure of the hand

The MCP joint of middle finger is the reference both in vertical and horizontal position. The horizontal distance between adjacent fingers is designed wider to avoid interference when fitted with glove. The index, the ring, and the little finger have rotary angles of 3°, 3°, and 6° around the axis of middle finger. The simulation experiments show that there is better envelope space because of the arches [10].

The opposability of the thumb is very important for dexterity and grasping stability. Two parameters are defined to describe it which are the oppose angle and the performance index. The oppose angle between the thumb and the middle finger is defined as ω, as shown in Fig. 2. It is designed to ensure the minimum distance larger than 95mm, By means of the anti-trigonometric equations (1), the value of ω can be calculated as 69°.

$$\begin{cases} \omega \geq \arccos(l_{ab}^2 + l_{bc}^2 - l_{ca}^2 / 2l_{ab}l_{bc}) \\ l_{ac} \geq 95 \end{cases} \quad (1)$$

Where l_{ab} is the length of thumb, l_{bc} is the length of the middle finger.

A performance index [11] of the thumb opposability is defined by (2).

$$J = \frac{1}{d^3} \sum_{i=1}^{k} w_i v_i \quad (2)$$

Where v_i denotes the volume of intersection between the mobility space of the thumb and that of the i-th finger, each v_i is the function of φ, and can be obtained by using the Mechanica module of Pro-E. k denotes the number of the finger except the thumb, d is the length of the thumb, and w_i is a weighting coefficient, simply, each w_i equals to 1.00. The bigger J becomes, the stronger the hand performs. According to the simulation results, the value of J reaches maximum, when φ is 28.6°.

B. Modular Design of Index, Mid, Ring, and Little Finger

Commercial prosthetic hands usually use fixed shape fingers which may bring two limitations: Firstly, the motion of the finger is unnatural; secondly, the sensory information is poor. In order to overcome these disadvantages, the physiology of human finger needs to be studied as discussed in [12]. Generally three aspects need to be considered: the actuation, the transmission, and the integration of sensors.

The multi-functionality of the prosthetic hand depends on the actuator's performance. We adopted a DC motor to drive the finger because it is more balanced in the efficiency, response time, and reliability. The actuation unit consists of a DC motor, a planetary gearheads and an incremental magnetic encoder. The specifications of each finger are shown in table I.

Parameters	Thumb	Index finger & Middle finger	Ring finger & Little finger
Operating angle	[-5° 40°]	[0° 87°]	[0° 87°]
Angular velocity	68 (°/s)	68 (°/s)	118 (°/s)
Motor power	1.3 (mN·m)	1.3(mN·m)	0.8 (mN·m)
Gearbox ratio	484:1	484:1	256:1
Fingertip force	10 (N)	10 (N)	4.3 (N)

TABLE I
SPECIFICATIONS OF EACH FINGER

Two groups of planar linkage mechanism were adopted in series to realize the transmission of power, so the whole finger is coupled. Compared to the underactuated linkage mechanism [13], it does not contain elastic parts which are a consumption of battery energy. In order to better imitate the shape of each finger in relax, an initial inflexed angel of 15° was adopted between proximal phalanx and medial phalanx, as shown in Fig. 3.
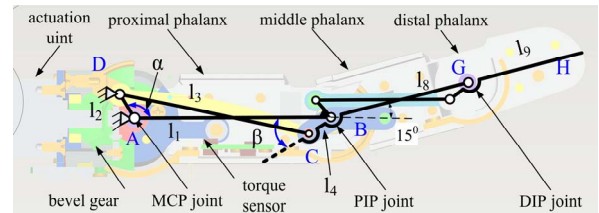

Fig. 3. The planar linkage mechanism

Where l_1 is the driving bar, l_2 is the seat, l_3 is the driven bar, l_4 is the transmission bar. l_4 is driven by l_1 through l_3 during grasp. Thus a close loop planar linkage mechanism is established. l_8 is the length of middle phalanx, l_9 is the length of distal phalanx, the transmission ratio between each phalanx is approximately 1:1. According to algebraic geometry, the length of l_3 is determined by (3).

$$l_3 = f_1(\alpha_0, \beta_0) \quad (3)$$

Where α_0 and β_0 are the initial angel of α and β.

The optimum values of α_0 and β_0 are determined according to δ, which is given by (4). When α changes from α_0 to ($\alpha_0 + 90^0$), the expected value of δ, denoted as $E(\delta)$ and the variance of δ, denoted as $D(\delta)$, are given by (5).

$$\delta = f_2(\alpha, \alpha_0, \beta_0) = (\alpha_0 - \alpha) - (\beta - \beta_0) \qquad (4)$$

$$E(\delta) = \sum_{k=1}^{n} \frac{\delta_k}{n} \qquad D(\delta) = \sum_{k=1}^{n} \frac{[\delta_k - E(\delta)]^2}{n} \qquad (5)$$

Where δ is the difference between $(\alpha_0 - \alpha)$ and $(\beta_0 - \beta)$; n is the number of samples in the range of α.

According to iterative calculation, when $E(\delta)$ is below $1°$ and $D(\delta)$ reaches the minimum, the values of α_0, β_0 and l_3 are determined. i.e. l_1=23mm, l_2 =4mm, l_4 =4mm. l_3= 22.01mm.

The kinematics analysis was carried out by taken the advantage of Assur Group theory. The planar mechanisms were divided into first order mechanism and class 2 Assur group. l_1 is the driving bar, $\alpha \in [0°, 87°]$, The trajectory of each joint show that the finger resembles like human finger, shown in Fig. 4.
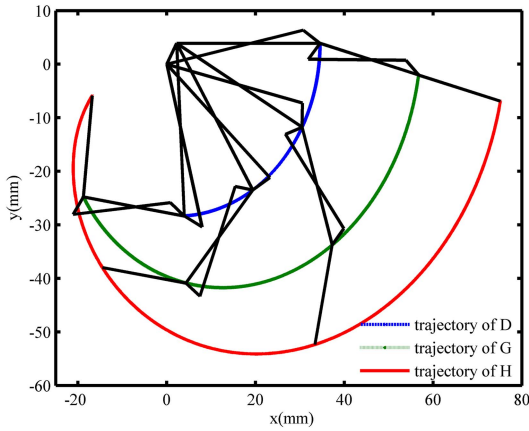

Fig. 4. The trajectory of each joint

The hand needs as a minimum a set of force and position sensors to enable intelligent control schemes. The position & torque sensors are embedded in the mechanical structure, as shown in Fig. 5.
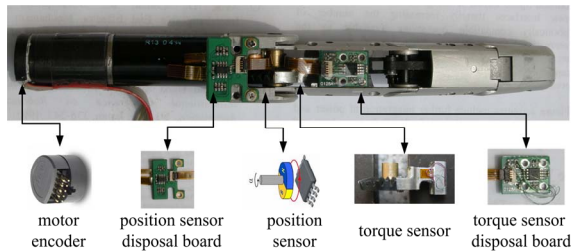

Fig. 5. Sensory configurations of the index finger

A Hall Effect sensor is applied to measure the position of MCP joint. Its measurement principle can be seen in [14]. The torque sensors are embedded in the finger structure. The measurement principle is based on the induced mechanical strains on elastomers. Shapes and dimensions of elastomers are determined by utilizing ANSYS FEM software. Two SR-4 strain gauges are implemented in the Wheatstone bridge processing circuit. Calibration of torque sensors is implemented when finger extended fully, the linearity

is $\pm 1.94\%$, the repeatability is $\pm 0.82\%$, and the hysteresis is $\pm 2.51\%$. The analog signals were converted to digital nearby to decrease electromagnetic disturbance. The sampling frequency of the A/D is 500Hz.

C. Characteristics of Thumb

The human's thumb usually inclines to the palm when relaxed and grasp along a cone surface, which is far different from that of most previous prosthetic hand [15]-[17].

Based on the position of thumb mentioned above, the geometry is specially designed to mimic the motion of human thumb when grasp. The metacarpal of the thumb is placed at 30º deflexion to the base joint of the middle finger. In addition, there is an initial abduction of 30º to the palm, as shown in Fig. 2. In order to realize such an effect, an RSRRR spatial linkage mechanism was designed, as shown in Fig. 6.
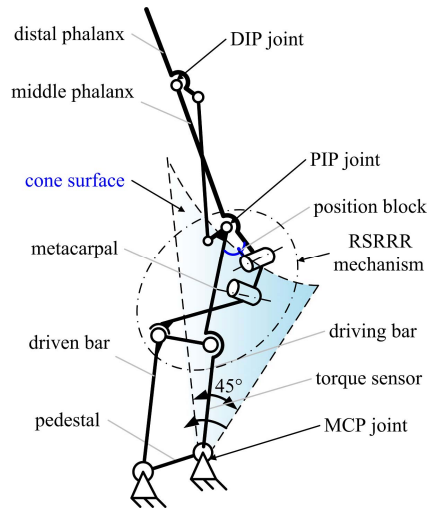

Fig. 6. Simple view of the thumb

By doing so, the planar finger motion is extended to three dimensional spaces. The last two joints are coupled as other four fingers. The workspace of thumb presents a cone surface, which is similar to human hand. The thumb, 85mm long, 17mm wide and 14mm thick, weighs about 80g.

III. HARDWARE ARCHITECTURE

The currently developed humanoid hand is controlled by multi-processor controller based on DSP. The architecture of the control system is shown in Fig. 7. The control system of the prosthetic hand is hierarchically organized [18]: a high-level supervisory controller is in charge of implementing EMG signal acquisition and pattern recognition. It plans movement task and presents a set of commands (e.g. the close, open and desired torque of the finger etc.) to a lower-level controller through controller area network (CAN) bus. The lower-level is designed to coordinate the movements of the fingers and accomplish grasp. The proposed control architecture is implemented on two boards, the motion control board and the signal processing board.

Besides, in order to realize the bio-feedback function, an

electrical stimulator is also designed. It consists of two parts: one is the electrode which adheres to skin directly; the other is electrical signal generator which is adopted to actuate the electrode. The electrical stimulator has six hierarchies. Each represents certain force level and is realized by adjusting the frequency of stimulation.
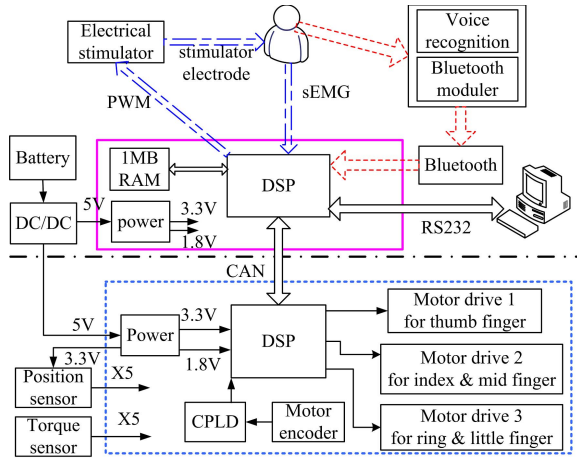

Fig. 7. The hardware architecture of control system

A. Motion Control Level

The core of motor control is realized by TMS320F2810, which is a kind of DSP produced by TI. It has 6 channel independent PWM (pulse width modulation) outputs. And each channel can control one DC motor. In addition, it has 16-channel 12 bit A/D converter to realize signal sampling from torque & position sensors and motor encoders. The direction of motors and pulse signals from encoder sent to DSP are acquired by CPLD (complex programming logic device). The control cycle is $800\,\mu s$. This frequency could allow us to control five fingers at the same time.

B. EMG Control Level

In order to realize the real-time control scheme, TMS320F2812 of TI is used in the EMG processing board. It is a new mix signal 32 bit digital signal processor (DSP) executing 150 MIPS (million instructions per second). Abundant port and 16 passage 12 bit analog-to-digital (A/D) converter are integrated on the chip to realize EMG signal sampling. The recognition method of hand gestures with support vector classification (C-SVC) is developed, which is implemented in the TMS320F2812 [19].

IV. PERFORMANCE OF THE PROSTHETIC HAND

The hand is controlled by EMG signals in real-time which can offer an extended physiological proprioception. Typically the steady state and the transient state EMG signals are combined in human grasp operations. However, the recognition of transient state is relatively low. In order to overcome this problem, we implemented a novel two-stage decision strategy. Besides, the position-based impedance control is implemented as the force control strategy.

A. EMG Data Acquisition

Six 13E200=50 electrodes [20], made by Otto Bock Company in Germany are utilized to record EMG signals. The electrodes are designed with a built-in filter and a built-in adjustable gain that can directly indicate the amplitude of muscle contraction. The muscles and the displacement of the EMG electrodes are determined by separating the signal generated by a muscle from that of its neighbors as clear as possible. The gesture mode was classified at first, that is, "1" means the finger motion to the extend position, "-1" means the motion to flex position and "0" means motion to middle position. The muscles and corresponding mode are shown in table II.

	Name of the muscle	Corresponding mode
1	Extensor pollicis brevis	Extend thumb (1,0,0)
2	Flexor pollicis longus	Flex thumb (-1,0,0)
3	Extensor indicis proprius	Extend index (0,1,0)
4	Flexor digitorum superficialis (distal)	Flex index (0,-1,0)
5	Extensor digiti quinti proprius	Extend rest (0,0,1)
6	Flexor digitorum superficialis (proximal)	Flex rest (0,0,-1)

TABLE II
THE RELATED MUSCLES AND CORRESPONDING BASIC MODES

B. EMG Pattern Recognition

The key point of the real-time sEMG control is how to classify different hand modes accurately; therefore we established a two-stage decision strategy. The first stage is for the discrimination of the idle and active modes; it is a simple threshold decision which is given by (6)

$$\begin{cases} f_1(x) = \text{sgn}(\sum_{i=1}^{6}(\text{sgn}(x(i)-Thd(i))+4) \\ f_1(x) = \begin{cases} 1 & \text{active} \\ -1 & \text{idle} \end{cases} \end{cases} \quad (6)$$

Where $x(i)$ is the sampling value of the EMG signal in channel i, $i = 1,2,3,...6$ and $Thd(i)$ is the channel's threshold (typically 1/5 of the EMG signal value scope within the channel). Refer to (6), if any channel's EMG signal is beyond its corresponding threshold, the hand gesture will be recognized as one of active modes.

The second stage is for the recognition between different active modes, i.e. m and n; it is conducted through SVM methods. The performance of SVM is depending upon the selection of kernel function, because the kernel function defines the feature space in which data are classified. According to previous research, The Radial Basis Function (RBF) kernel is chosen [21], [22]. The kernel function is given by (7).

$$K(x_i, x_j) = \exp(-\gamma \|x_i - x_j\|^2) \quad (7)$$

Where γ is the kernel parameter, $\gamma > 0$

By taken the advantage of Lagrange optimal method, the optimal hyperplane can be transformed into dual problem. Hence, the indicator function is now given by (8).

$$\begin{cases} f(x) = sgn\left[\sum_{i=1}^{l} \alpha_i y_i K(x_i, x) + b\right] \\ f(x) = \begin{cases} 1 & \text{active mode m} \\ -1 & \text{active mode n} \end{cases} \end{cases} \quad (8)$$

Where α_i is the Lagrange multipliers, the upper bound is C, for those $\alpha_i > 0$ are called "support vectors"; x, x_i are vectors; y_i are labels, might be -1 or 1; b is the threshold.

We use one-against-one method to solve multi-modes' classification. For the regression operation, we use epsilon-SVR method, also RBF kernel function. For the optimization of a pair of parameters, the penalty parameter C and kernel function coif gamma, we will make a grid research combined with cross-validations.

C. Position-Based Impedance Control Scheme

Position-Based Impedance Control (PBIC) scheme is applied to obtain better adaptability of force control. Target dynamic model of the finger joint can be specified by a generalization of a second order dynamics of a damped spring

$$M_d(\ddot{\theta}_r - \ddot{\theta}) + B_d(\dot{\theta}_r - \dot{\theta}) + K_d(\theta_r - \theta) = T \quad (9)$$

Where K_d, B_d, M_d are the target desired stiffness, environmental damp and inertial matrix, θ is the actually angle of finger joint, θ_r is the reference angle of finger joint, and T is the actual reaction force that the environment exerts on the finger. Because there is only one active joint of the finger, K_d, B_d, M_d are monomials. As the speed of the finger is slow, M_d is neglected. According to previous results [23], the most crucial parameter for contact stability is the target damping ratio B_d. Therefore, an outer loop independence controller containing K_d, B_d is designed, as shown in Fig. 8.
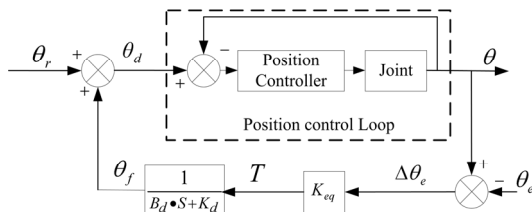

Fig. 8. Position-based impedance controller

The position controller provides the basis of the implementation of the PBIC scheme. An incremental PID controller was applied as the position controller. A model of this system is given by the following set of equations

$$\begin{cases} \Delta U(k) = \left\{ K_P \Delta\theta(k) + K_d \Delta\dot{\theta}(k) + K_I \theta_e(k) \right\} \\ \Delta\theta(k) = \left[\theta_e(k) - \theta_e(k-1) \right] \\ \Delta\dot{\theta}(k) = \left[\theta_e(k) - 2\theta_e(k-1) + \theta_e(k-2) \right] \end{cases} \quad (10)$$

Where $\theta_e = \theta_r - \theta$ is the position error; θ_r, θ, and ΔU are the desired position, actual position, and controller output, respectively. In the experiment, K_P is 1.5, K_I is 0.02, K_d is

0.5.

D. Experiment Result

To verify the effectiveness of the system and proposed sEMG control strategy, a set of grasp operations combing PBIC scheme are conducted. Our experiments show that, the decision frequency of current hand gesture can reach to 10Hz in 18 modes and 40Hz in 9 modes, which is sufficient for real time control of the hand with a maximum time delay of 100 ms. The success rate of 10 modes is up to 90%. Fig. 9 shows that the finger tracks the desired trajectory with the maximal error of no more than 0.35 degree in free space, while in contact the desired position changes, with a proper value of B_d =0.6 $Nm/rad/s$, the finger quickly stabilized in the new position with a tiny overshoot. After disengagement, the finger quickly follows the designed trajectory in free space.
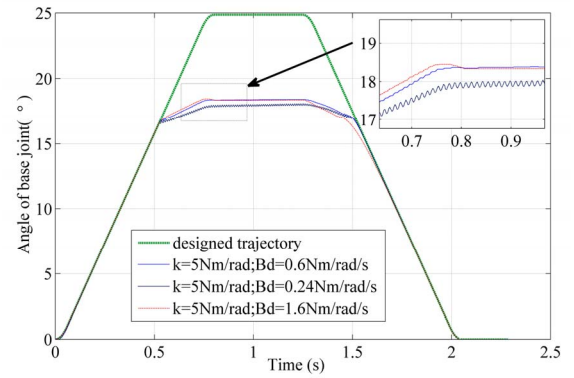

Fig. 9. Position response of PBIC control result

Fig. 10 shows that the torque changes correspond to the position. The initial value of the torque sensor is not zero; this may be caused by the friction of the mechanism. It also shows that with B_d =0.24 $Nm/rad/s$, the grasp is unstable, whereas with B_d =1.6 $Nm/rad/s$, a big overshoot appears.
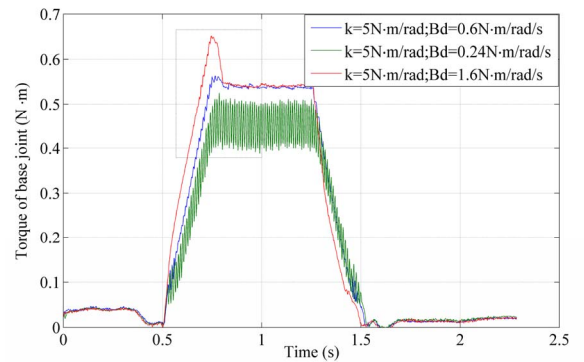

Fig. 10. Torque response of PBIC control result

According to the results, we can see that the humanoid hand, which is controlled by EMG signals, will swiftly follow the instruction hand (human hand) to move its relative fingers to hold the object steady, as shown in Fig. 11. The hand can perform pinch, three jaw chawk, and cylinder grasp.

The proposed control scheme can be adopted in the control of multi-DOF prosthetic hands and other life-like artificial appendages, such as limbs, legs, and foot.
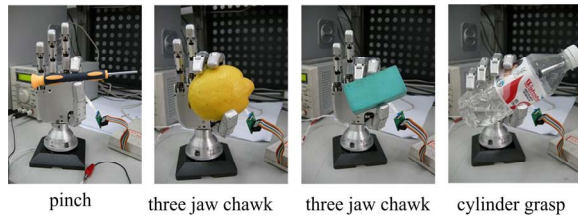
| pinch | three jaw chawk | three jaw chawk | cylinder grasp |

Fig. 11. Grasp modes of the hand

V. CONCLUSIONS AND FUTURE WORK

The concept of the novel anthropomorphic prosthetic hand and an intuitive control scheme via forearm surface EMG signals are presented. The hand has cambered palm and five active fingers. Each finger is integrated with position and torque sensors. This feature offers the hand more grasping patterns and complex control methods. On the other hand, by a novel two stage decision strategy; the hand can be controlled by sEMG signals in the real-time. This feature enables the hand to respond seamlessly to the intent of human user. There may be some prosthetic hands that have more DOFs or more sensors, but considering the small size, low weight, human-like cosmetics, biomimetic controllability and perception in all; the hand that we developed is more capable of being an intimate extension of human body.

The prosthetic hand can be applied in two aspects. Firstly, it can be treated as an end operator of a multi-DOF robot arm to interact with the environment. Second, with a human like glove, it can be utilized for the prosthetic uses.

Future work will focus on experiments with different EMG control strategies. The bio-feedback control strategy is being researched, which will communicate a sense of touch back to the user. Besides, we are now trying to evaluate a novel control method base on Force Sensitive Resistors (FSR) sensors, which is cheap and stable.

REFERENCES

[1] "Otto Bock myoelectric arm prostheses." [Online]. Available: http://www.ottobock.com/cps/rde/xchg/ob_com_en/hs.xsl/384.html.

[2] C. Pylatiuk, S. Mounier, A. Kargov, S. Schulz, G. Bretthauer, "Progress in the development of a multifunctional hand prosthesis," *26th IEEE Annual Int. Conf. on Engineering in Medicine and Biology Society*, San Francisco, USA, 2004, pp. 4260–4263.

[3] L. Zollo, S. Roccella, R. Tucci, B. Siciliano, "Biomechatronic design and control of an anthropomorphic artificial hand for prosthetics hand robotic applications," *Biorob2006*, Pisa, Italy, Aug. 2007, no. 4, pp. 418–429.

[4] A. M. Dollar and R. D. Howe, "The SDM hand as a prosthetic terminal device: a feasibility study," *in Proc. 2007 IEEE Int. Conf. on Rehabilitation Robotics*, The Netherlands, 2007, pp. 978–983.

[5] C. Cipriani, M. Controzzi, and M. C. Carrozza, "Progress towards the development of the smarthand transradial prosthesis," *2009 IEEE Inter. Conf. on Rehabilitation Robotics*," Japan, 2009, pp. 682–687.

[6] J. L. Pons, E. Rocon, and R. Ceres, "The MANUS-HAND dextrous robotics upper limb prosthesis: mechanical and manipulation aspects," *Autonomous Robots*, vol. 16, no. 2, pp. 143–163, March 2004.

[7] J. D. Zhao, Z. W. Xie, L. Jiang and H. G. Cai, "Levenberg-Marquardt based neural network control for a five-fingered prosthetic hand, " *in Proc. 2005 IEEE Int. Conf. on Robotics and Automation*, Barcelona, 2005, pp. 4482–4487.

[8] J. D. Zhao, Z. W. Xie, L. Jiang, and H. G. Cai, "EMG control for a five-fingered prosthetic hand based on wavelet transform and autoregressive model," *Proc. of the 2006 IEEE Int. Conf. on mechatronics and automation*, Luoyang, China, 2006, pp. 1097–1102.

[9] A. P. Sangole, M. F. Levin, "Arches of the hand in reach to grasp," *Journals of Biomechanics*, vol. 41, pp. 829-837, 2008.

[10] O. J. Lewis, "Joints remodeling and the evolution of the human hand," *Journal of Anatomy*, pp. 157-201, 1977.

[11] M. Tetsuya, K. Haruhisa, and Y. Keisuke, "Anthropomorphic robot hand: Gifu hand III," *ICCAS2002*, pp. 1288–1293.

[12] F. H. Netter, *Atlas of Human Anatomy, Second Edition*. Icon Learning Systems, Teterboro, New Jersey, 1997.

[13] B. Massa, S. Rosella, M. C. Carrizozo, and P. Dario, "Design and development of an underactuated prosthetic hand," in *Proc. of the 2002 IEEE Int. Conf. on Robotics and Automation*,Washington. DC, 2002, pp. 3374–3379.

[14] X. H. GAO, M. H. Jin, L. Jiang, Z. W. Xie, P. He, L. Yang, Y. W. Liu, R. Wei, H. G. Cai, H. Liu, J. Butterfass, M. Grebenstein, N. Seitz, G. Hirzinger, "The HIT/DLR dexterous hand: work in progress," in *Proc. of IEEE Int. Conf. on Robotics and Automation*, 2003, pp. 3164–3168.

[15] L. Biagiotti, F. Lotti, C. Melchiorri, and G. Vassura, "Mechatronic design of innovative fingers for anthropomorphic robot hands," in *Proc. of the 2003 IEEE Inter. Conf. on Robotics and Automation*, 2003, vol. 3, pp. 3187–3192.

[16] S. Schulz, C. Pylatiuk, and G. Bretthauer, "A new ultralight anthopmorphic hand," in *Proc. of the 2001 IEEE Int. Conf. on Robotics and Automation*, Seoul, Korea, May. 2001, pp. 2437–2441.

[17] D. Rajiv, Y. Clement, and L. Maurice, "The design and development of a gloveless endoskeletal prosthetic hand," *Journal of Rehabilitation Research and Development*, vol. 35, no. 4, pp. 388–395, 1998.

[18] P. J. Kyberd and J. L. Pons, "A comparison of the Oxford and Manus intelligent hand prostheses," in *Proc. of IEEE Int. Conf. on Robotics and Automation*, 2003, vol. 3, pp. 3231–3236.

[19] D. P. Yang, J. D. Zhao, L. Jiang, H. Liu, "EMG control of a 3-DOF anthropomorphic prosthetic hand," *Journal of Jiangsu University (Nature Science Edition)*, vol. 30, no. 1, pp. 05–09, Jan. 2009(in Chinese).

[20] "Otto Bock MYOBOCK 13E200=50 electrodes." [Online]. Available: http://www.ottobockus.com/products/upperlimbprosthetics/myoelectric hands myobockr.asp.

[21] S. S. Keerthi and C. J. Lin, "Symptotic behaviors of support vector machines with Gaussian kernel," *Neural Computation*, vol. 15, no. 7, pp. 1667–1689, 2003.

[22] C. Castellini and P. van der Smagt, "Surface EMG in advanced hand prosthetics," *Biological Cybernetics*, vol, 100, no. 1, pp. 35–47, 2009.

[23] D. Surdilovic, "Contact stability issues in position based impedance control: theory and experiments," in *Proc. of IEEE Int. Conf. on Robotics and Automation*, 1996, pp. 1675–1680.